Structure and dynamics of the Andean margin: Insights from a 3D density model (5°-45°S)

Andrés Tassara [1], Hans-Jürgen Götze [2], & Sabine Schmidt [2]

1 Institut für Geologische Wissenschaften, Freie Universität Berlin, Germany (andres@geophysik.fu-berlin.de)
2 Institut für Geowissenschaften, Christian-Albrechts-Universität Kiel, Germany

Introduction

The active western margin of South America is characterized by a remarkable along-strike segmentation whose causes are not yet understood. Several authors argue that the observed correlation between features of the oceanic Nazca plate at the trench, the shape of the subducted slab and boundaries of Andean segments imply that this segmentation is primarily controlled by the current configuration of the subducting plate (e.g. Nur and Ben-Avraham, 1981; Jordan et al., 1983; Pardo Casas and Molnar, 1987; Yáñez and Cembrano, 2004). However, the Andean segmentation is a long-term (10^8 yr) geological feature (e.g. Mpodozis and Ramos, 1989; Kley et al., 1999) that cannot be exclusively explained in terms of the subducting plate configuration because it changes at short time-scales (10^6-10^7 yr) during plate reorganizations: The old structure of the continent should also play a role in controlling the fate of the Andean margin and the maintenance of its segmentation. The evaluation of this hypothesis requires a minimal knowledge of the compositional-rheological structure of the Andean lithosphere that we tried to fulfil by forward modelling of the Bouguer anomaly for a region of the Andean margin between 5° to 45°S and 60° to 85°W. This exercise resulted in a three-dimensional (3D) model describing the density structure of the Nazca plate, the subducted slab and the continental lithosphere (Tassara et al., submitted paper). In this contribution we discuss some possible geodynamic implications of this model.

Method and data

We forward modelled the Bouguer anomaly (onshore data provided by D. Blitzkow, Universidade de São Paulo-Brazil; offshore data from KMS global free-air anomaly) using the software IGMAS (Schmidt and Götze, 1998) and triangulating between 43 vertical cross-sections separated by 1°. This method generates a 3D density model at regional to continental scales.
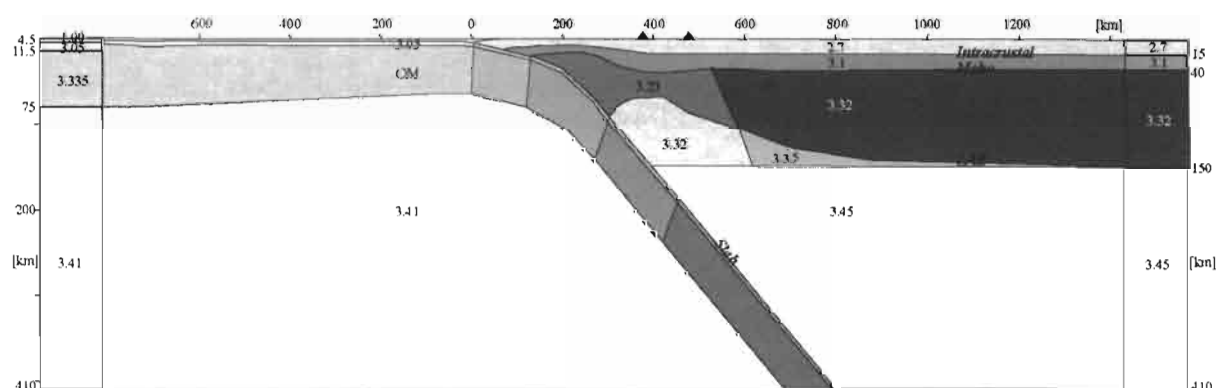

Fig.1: Density structure of the 43 vertical cross-sections forming the 3D model. 2-times vertical exaggeration. Values are in Mg/m³. The figure doesn't show values of: 1) oceanic mantle (OM), which varies along the modelled region from 3.26 (45°S, 10My old) to 3.355 (20°S, 45My old); 2) bodies forming the subducted slab, increasing from values of the oceanic plate at the trench to 3.7 (deepest oceanic crust) and 3.55 (deepest oceanic mantle). Columns along figure's extremes represent the reference model. This reference model is that expected for both a continental shield conducting a heat flow of 50 mW/m² (right) and an oceanic lithosphere 30 My old (left). Triangles are volcanoes. Names in bold-italics label the four main density discontinuities beneath the continent whose resulting geometries are shown in Fig. 2.

The structure of each cross-section is shown in Fig. 1. Densities were selected after studying the relationship between this parameter and composition, pressure-temperature conditions and water content of crustal and mantle materials. The geometry of the subducted slab was fixed using an updated seismic-seismological database that compiles earthquake hypocenters recorded at local and teleseismic distance, refraction-reflection seismic profiles, receiver function analyses and global tomography models. The continental Moho was locally constrained by results of receiver function analyses and Pn apparent phase velocities. Tassara et al. (submitted paper) describe the details concerning the location and source of these data. The Bouguer anomaly along each section was compared against a modelled anomaly that is calculated from the density contrast between the user-defined density structure and a reference model. Iteratively changing this structure, we obtained a standard deviation of 15.5 mGal between measured and modelled anomalies.

Results and discussion

Fig. 2 shows the final geometry resulting from the forward gravity modelling for the density discontinuities underneath the continent labelled in Fig. 1. We analyse these geometries and discuss some topics relevant to Andean geodynamics.

Subduction of oceanic ridges and causes of slab segmentation. Fig. 2a shows the geometry of the subducted slab along with contour lines for the Nazca crustal thickness resulting from the model. South of 10°S, the Peruvian flat-slab is evident at around 100 km depth, is relatively narrow and has a morphology controlled by the subduction of the huge Nazca ridge (continuous crustal root >20 km thick). North of 10°S, the flat segment is 100 km broader and 20 km deeper and its morphology is correlated with surface topography. The latter has characteristics similar to those of the Argentinean flat-slab that seems to be associated along its southern termination (~32.5°S) with the prolongation of the Juan Fernández ridge, which has a discontinuous crustal root thinner than 15 km. The subduction of the Iquique ridge, having a more continuous crustal root, is associated with a steeply subducting slab. These observations suggest that the positive buoyancy of subducted ridges with respect to the surrounding slab is a necessary but insufficient condition for causing slab flattening. Other factors to be considered are the locally enhanced hydration of the uppermost oceanic mantle (Kopp et al., 2004) and particularly the dynamic control exerted by the absolute westward motion of the South American plate (e.g. van Hunen et al., 2004) coupled with along-strike variations in the amount of convergence absorbed by crustal shortening.

Forearc structure, seismogenic zone and mass transfer modes. Fig. 2c shows the modelled intersection of the continental Moho with the subducted slab along the Central Andes (5°-33°S) laying at a depth of 30-50 km, which correlates with the downdip limit of the seismogenic zone (DLS) after Khazaradze and Klotz (2003). In this case our model supports Oleskevich et al. (1999), in that this limit is controlled by the point where the slab encounters hydrated forearc mantle. However, South of 35°S the modelled intersection is 100 km westward from and 20 km shallower than the DLS, which further correlates with the 40-50 km contour of the subducted slab (Khazaradze and Klotz, 2003). This could imply that the mantle beneath the Southern Andean forearc is likely not hydrated enough to preclude stick-slip seismogenic behaviour. Figs. 2c and 2d also reveal that between 15° and 35°S, the forearc Moho is relatively flat and the entire forearc is dominated by mafic crust (intracrustal discontinuity ICD <5 km) contrasting with the situation outside this region where the offshore forearc is

719

dominated by felsic material (ICD >10 km) and the Moho shallows below the coastline north of 15°S and along the Central Valley south of 38°S. These variations in forearc structure and composition are correlated with surface geology and should control, at least partially and in a way still to be determined, the contrasting mass transfer modes along the margin (erosive between 15° and 35°S, neutral to accretive northward and southward).

Volcanic arcs. The Central (CVZ) and Southern (SVZ) volcanic zones of the Andes are underlain by lithosphere thinner than 80 km, with values lower than 60 km below the northern Puna (24°S) and south of 36°S along the SVZ (Fig. 2b). The front of the CVZ lies 100-120 km above the subducted slab (Fig. 2a) and is constructed on a crust thicker than 60 km (except under the Puna, Fig. 2c) characterized by ICD >15 km (Fig. 2d) that suggests an important felsic component in the crustal composition. The depth to the slab decreases south of 37°S along the SVZ down to values of ~75 km south of 40°S; the crustal thickness also decrease from 60 km at the northern SVZ till less than 30 km along the southernmost SVZ. The basement of the SVZ south of 36°S seems to be dominated by a mafic crustal composition (ICD <10 km). The contrasting lithospheric and crustal nature between the CVZ and SVZ and the coupled along-strike changes along the SVZ are likely the main causes behind the distinctive geochemical signature of Andean volcanic zones (e.g. Hildreth and Moobarth, 1988). The scale and resolution of our model should be adequate to perform a systematic analysis relating the geometry of the subducted plate and the structure and composition of the continental lithosphere with magmagenetic processes responsible for the nature and evolution of Andean volcanic arcs.

Lithospheric structure and deformation mechanisms of the continental margin. The geodynamic evolution of the Andean margin is dominated by Neogene crustal shortening along the Central Andes and no-shortening to extension along the Southern Andes (e.g. Mpodozis and Ramos, 1989). What controls this contrasting evolution? The LAB below the Altiplano-Puna plateau (15°-28°S) being shallower than 100 km in our model (Fig. 2b), suggests a thermally weakened lithosphere that promotes concentration of compressive deformation. However, the lithosphere of the Southern Andean back-arc is extremely thin (<80 km) and yet it is not associated with crustal shortening. We suspect that the primary control on orogenic evolution is exerted by the internal crustal structure accompanying thermal weakening: the felsic component of the Central Andean orogen (ICD >15 km) makes the crust rheologically weaker than the mafic-dominated Southern Andes (ICD <10 km) likely controlling their contrasting response to the external stress field. In addition, variations of ICD along the Central Andes correlates with changing foreland deformation mechanisms; a shallower ICD along the central Altiplano coincides with the flat detachment of the thin-skinned Sierras Subandinas, whereas toward the boundaries of the plateau, a deeper ICD coincides with thick-skinned deformation styles (Kley et al., 1999). This and the crustal thickness distribution could indicate an upper-lower crustal decoupling and lower crustal flow of likely molten mafic material toward the center of the plateau as envisaged by Hindle et al. (2005).

References

Hildreth, W; S. Moobarth. 1988. *Contr. Min. Petrol.* 98, p 455-489.
Hindle, D; J. Kley; O. Oncken; S. Sobolev. 2005. *Earth Planet. Sci. Lett.* 230, p 113-124
Jordan, T; B. Isacks; R. Allmendinger; J. Brewer; V. Ramos; C. Ando. 1983. *Geol. Soc. Am. Bull.* 94, p 341-361
Khazarndze, G; J. Klotz. 2003. *Jour. Geoph. Res.* 108 B6, doi:10.1029/2002JB001879
Kley, J; C. Monaldi; J. Salfity. 1999. *Tectonophysics* 301, p 75-94
Kopp, H; E. Flueh; C. Papaenberg; D. Klaeschen. 2004. *Tectonics* 23, doi:10.1029/2003TC001590
Mpodozis, C; V. Ramos. 1989. in *Geology of the Andes and its relation to hydrocarbon and mineral resources*, Ericksen, Cañas-Pinochet and Reinemund Eds.. Earth Sci. Series, p 59-90.
Nur, A; Z. Ben-Avraham. 1981. *Geol. Soc. Am. Mem.* 154, p. 729-740.
Oleskevich, D; R. Hyndman; K. Wang. 1999. *Jour. Geoph. Res.* 104, p. 14965-14991.
Pardo-Casas, F; P. Molnar. 1987. *Tectonics* 6 N3, p. 233-248.
Schmidt, S; H-J. Götze. 1998. *Phys. Chem. Earth* 23, p. 289-295.
Tassara, A; H-J. Götze, S. Schmidt. Paper submitted for the Final Report of the SFB267 project "Deformation Processes in the Andes"
van Hunen, J; A. van den Berg; N. Vlaar. 2004. *Phys. Earth Plan. Int.* 146, p 179-194.
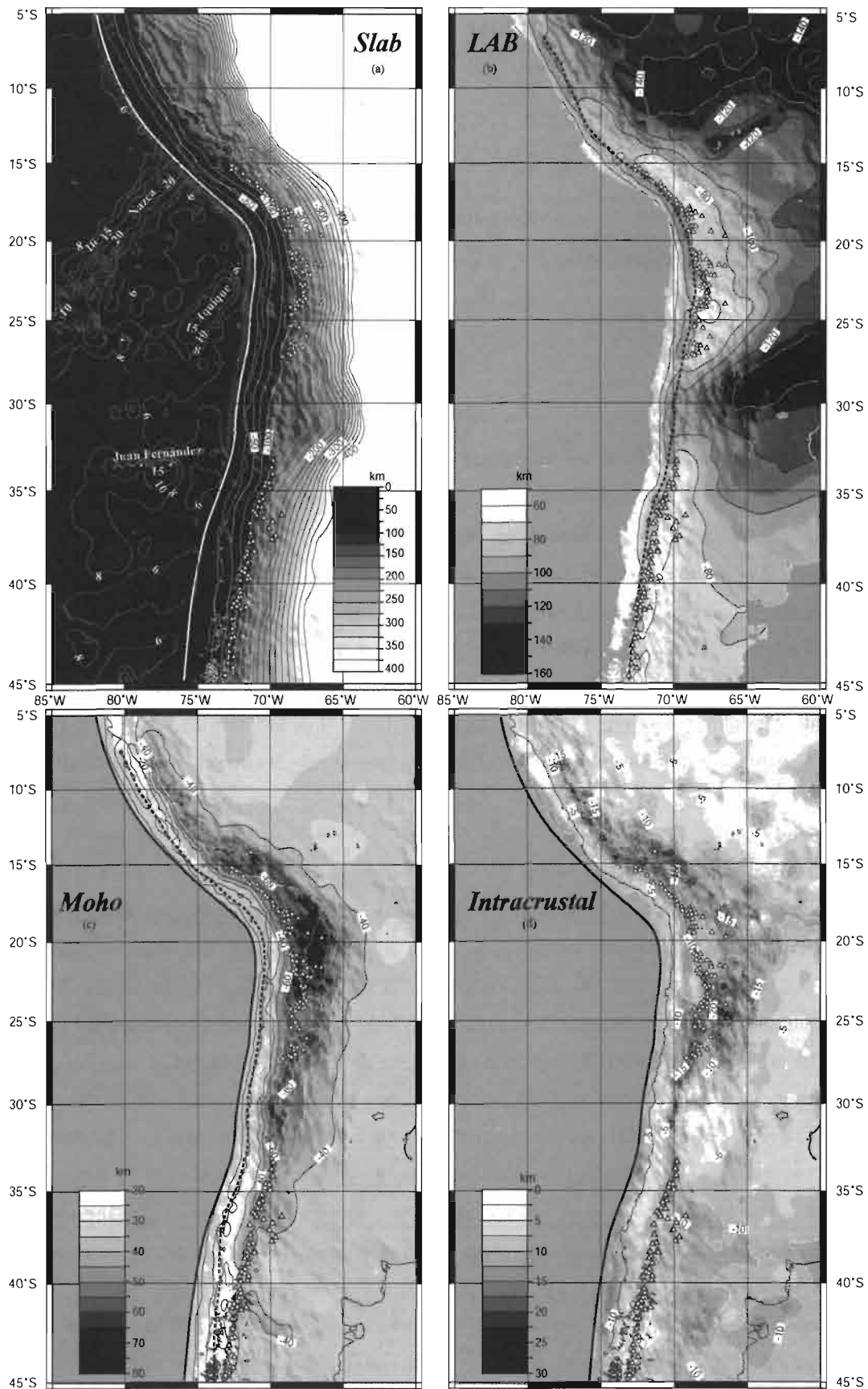Yáñez, G; J. Cembrano. 2004. *Jour. Geoph. Res.* 109, doi:10.1029/2003JB002494

Fig. 2. Geometries of density discontinuities underneath the continent resulting from the forward gravity modelling. Triangles are active volcanoes (http://www.volcano.si.edu/world). Thick line is the trench axis. a) subducted slab, contour lines offshore denote oceanic crustal thickness; b) lithosphere-astenosphere boundary, segmented line is the intersection with the slab; c) continental Moho, segmented line is the intersection with the slab; d) intracrustal discontinuity. Figures are shaded with topography to observe correlation with morphostructure.